Optical Flow and Image Registration : a New Local Rigidity Approach for Global Minimization

Martin Lefébure[1] and Laurent D. Cohen[2]

[1] Current address: 69 rue Perronet, 92200 Neuilly Sur Seine, France, was with Poseidon Technologies. Email: mlefebure@compaqnet.fr
[2] CEREMADE, Université Paris-Dauphine, 75775 Paris cedex 16, France, cohen@ceremade.dauphine.fr

Abstract. We address the theoretical problems of optical flow estimation and image registration in a multi-scale framework in any dimension. Much work has been done based on the minimization of a distance between a first image and a second image after applying deformation or motion field. We discuss the classical multiscale approach and point out the problem of validity of the motion constraint equation (MCE) at lower resolutions. We introduce a new local rigidity hypothesis allowing to write proof of such a validity. This allows us to derive sufficient conditions for convergence of a new multi-scale and iterative motion estimation/registration scheme towards a global minimum of the usual nonlinear energy instead of a local minimum as did all previous methods. Although some of the sufficient conditions cannot always be fulfilled because of the absence of the necessary a priori knowledge on the motion, we use an implicit approach. We illustrate our method by showing results on synthetic and real examples (Motion, Registration, Morphing), including large deformation experiments.
Keywords:motion estimation, registration, optical flow, multi-scale, motion constraint equation, global minimization, stereo matching

1 Introduction

Registration and motion estimation are one of the most challenging problems in computer vision, having uncountable applications in various domains [17, 18, 6, 4, 13, 30]. These problems occur in many applications like medical image analysis, recognition, visual servoing, stereoscopic vision, satellite imagery or indexation. Hence they have constantly been addressed in the literature throughout the development of image processing techniques. For example (Figure 1) consider the problem of finding the motion in a two-dimensional images sequence. We then look for a displacement $(h_1(x_1, x_2), h_2(x_1, x_2))$ that minimizes an energy functional:

$$\int\int |I_1(x,y) - I_2(x + h_1(x,y), y + h_2(x,y))|^2 dxdy.$$

Next consider the problem of finding $(f_1(x_1, x_2), f_2(x_1, x_2))$ a rigid or non rigid deformation between two images (Figure 2), minimizing an energy functional:

$$\int\int |I_1(x,y) - I_2(f_1(x,y), f_2(x,y))|^2 dxdy.$$

Although most papers deal only with motion estimation or matching depending on the application in view, both problems can be formulated the same way and be solved with the same algorithm. Thus the work we present can be applied both to registration for a pair of images to match (stereo, medical or morphing) or motion field / optical flow for a sequence of images. In this paper we will focus our attention on these problems assuming grey level conservation between both images to be matched. Let us denote by $I_1(x)$ and $I_2(x)$ respectively the study and target images to be matched, where $x \in D = [-M, M]^d \subset \mathbb{R}^d$, and $d \geq 1$. In the following I_1 and I_2 are supposed to belong to the space $C_0^1(D)$ of continuously differentiable functions vanishing on the domain boundary ∂D. We will then assume there exists a homeomorphism f^* of D which represents the deformation such that:

$$I_1(x) = I_2 \circ f^*(x), \forall x \in D.$$

In the context of optical flow estimation, let us denote by h^* its associated motion field defined by $h^* = f^* - Id$ on D. We thus have:

$$I_1(x) = I_2(x + h^*(x)). \tag{1}$$

h^* is obviously a global minimum of the nonlinear functional

$$E_{NL}(h) = \frac{1}{2}\int_D |I_1(x) - I_2(x + h(x))|^2 dx. \tag{2}$$

We can deduce from (1) the well known Motion Constraint Equation (also called Optical Flow Constraint):

$$I_1(x) - I_2(x) \simeq < \nabla I_2(x), h^*(x) > , \forall x \in D. \tag{3}$$

Fig. 1. Finding the motion in a two-dimensional images sequence

E_{NL} is classically replaced in the literature by its quadratic version substituting the integrand with the squared difference between both left and right terms of the MCE, yielding the classical energy for the optical flow problem:

$$E_L(h) = \frac{1}{2}\int_D |I_1(x) - I_2(x) - < \nabla I_2(x), h(x) > |^2 dx.$$

Here ∇ denotes the gradient operator. Since the work of Horn and Schunk [17], MCE (3) has been widely used as a first order differential model in motion estimation and registration algorithms. In order to overcome the too low spatio-temporal sampling problem which causes numerical algorithms to converge to the closest local minimum of the energy E_{NL} instead of a global one, Terzopoulos et al. [24, 30] and Adelson and Bergen [8, 29] proposed to consider it at different scales. This led to the popular coarse-to-fine minimizing technique [18, 11, 13, 25, 14]. It is based on the remark that MCE (3) is a first order expansion which is generally no longer valid with h^* searched for. The idea is then to consider images at a coarse resolution and to refine iteratively the estimation process.

Using a regularizing kernel G_σ at scale σ, Terzopoulos et al. [24, 30] and Adelson and Bergen [8] were led to consider the following modified MCE:

$$G_\sigma * (I_1 - I_2)(x) \simeq < G_\sigma * \nabla I_2(x), h^*(x) > \tag{4}$$

Remark.
One could also consider regularizing both left and right terms of the original MCE, yielding the following alternative:

$$G_\sigma * (I_1 - I_2)(x) \simeq G_\sigma * (< \nabla I_2, h^* >)(x)$$

At finest scales it can be shown that these two propositions are equivalent.
To our knowledge and despite the huge literature on these approaches, no theoretical error analysis can be found when such approximations are done. Though it has been reported from numerical experiments that the modified MCE was not performing well at very coarse scales, thus betraying its progressive lack of sharpness, many authors pointed out convergence properties of such algorithms towards a dominant motion in the case of motion estimation [7, 11, 10, 21, 9, 16], or an acceptable deformation in the case of registration [13, 25, 26], even if the initial motion were large. It is widely assumed that deformation fields have some continuity or regularity properties, leading to the addition of some particular regularizing terms to the quadratic functional [17, 5, 30, 3, 2]. Let us emphasize on the modified MCE (4). We note $\hat{h}$ the value of h that reaches minimum for energy

$$\int |G_\sigma * (I_1 - I_2) - < G_\sigma * \nabla I_2, h > |^2 dx. \tag{5}$$

This multiscale approach assumes that Eqn. (4) is "valid" at lower resolutions, which ensures that $\hat{h}$ will be close to h^*.

Although it may come from the fact that flattened images are always "more similar", to our knowledge and despite the huge literature, no theoretical analysis can confirm this. Replacing G_σ by a particular low pass filter Π_σ (here

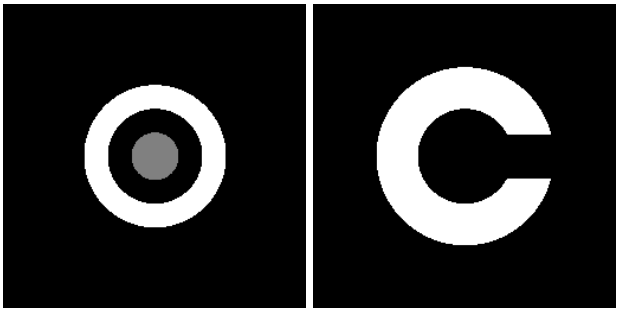

Fig. 2. Finding a non rigid deformation between two images

$\sigma \geq 0$ is proportional to the number of considered harmonics in the Fourier decomposition), we will address the problem of finding a linear operator $P_\sigma^{I_1}$ such that $P_\sigma^{I_1}(h^*)$ is close to $\Pi_\sigma\left(I_1 - I_2\right)$. The sharpness of this approximation will decrease with respect to both h^* norm and resolution parameter σ. This will lead us to introduce a new local rigidity hypothesis of deformations $f = Id + h$ with respect to image I_1. Hence such deformations allow to find the operator $P_\sigma^{I_1}$ satisfying our validity constraint on the modified MCE.

Considering general linear parametric motion models for h^*, we give sufficient conditions for asymptotic convergence of the sequence of combined motion estimations towards h^* together with the numerical convergence of the sequence of deformed templates towards the target I_2. Roughly speaking, the shape of the theorem will be the following:
Theorem: If

1. at each step the residual deformation is "locally rigid", and the associated motion can be linearly decomposed onto an "acceptable" set of functions the cardinal of which is not too large with respect to the scale,
2. the initial motion norm is not too large, and the systems conditionings do not decrease "too rapidly" when iterating,
3. the estimated deformations $Id + \hat{h}_i$ are invertible and "locally rigid",

Then the iterative scheme "converges" towards a global minimum of the energy E_{NL}.
The outline of the paper is as follows. In Section 2 we introduce a new local rigidity hypothesis and a low pass filter in order to derive a new MCE of the type of equation (6). In Section 3 we design an iterative motion estimation/registration scheme based on the MCE introduced in Section 2 and prove a convergence theorem. In order to avoid the a priori motion representation problem, we adopt an implicit approach in Section 4 and constrain each estimated deformation $Id + \hat{h}_i$ to be at least invertible. We show numerical results for large deformations problems in dimension 2. Section 5 gives a general conclusion to the paper.

2 Valid Modified MCE upon a new Local Rigidity Hypothesis

Assuming a local rigidity hypothesis and adopting the Dirichlet low-pass operator Π_σ, we will find a different right hand side featuring a "natural" and unique linear operator $P_\sigma^{I_1}$ in the sense that:

$$\Pi_\sigma(I_1 - I_2)(x) \simeq P_\sigma^{I_1}(h^*)(x), \tag{6}$$

with remainder of the order of $\|h^*\|^2$ for some particular norm and vanishing as the scale is coarser (σ close to 0).

2.1 Local rigidity property

In this paragraph we introduce our local rigidity property of deformations. Notations in this context are to be understood as follows:

- $D = [-M, M]^d$ in $\mathbb{R}^d$.
- $I_{1,p}$, $I_{2,p}$, I_2, are functions from $\mathbb{R}^d$ to $\mathbb{R}$.
- $h(x)$, $\tilde{h^*}(x)$ are functions from $\mathbb{R}^d$ to $\mathbb{R}^d$.
- $< .,. >$ denotes the scalar product in $\mathbb{R}^d$.
- $[.,.]$ denotes the scalar product in L^2.

For technical reasons we assume that I_1 and I_2 belong to $C_0^1(D)$, and $I_1(x) = I_2(x + h^*(x))$, $x \in D$, $h^*(x) \in \mathbb{R}^d$.

Definition 1. *$f \in Hom(D)$ is ξ-rigid for $I_1 \in C^1(D)$ iff:*

$$Jac(f)^t.\nabla I_1 = det(Jac(f))\nabla I_1, \tag{7}$$

where $Jac(f)$ denotes the Jacobian matrix of f and $det(A)$ the determinant of matrix A, and $Hom(D)$ the space of continuously differentiable and invertible functions from D to D (homeomorphisms).

All ξ-rigid deformations have the following properties (see [19] for the proofs). Assume f^* is ξ-rigid for $I_1 \in C_0^1(D)$ and $I_1 = I_2 \circ f^*$. Then,

1. equation (7) is always true if dimension d is 1;
2. for all $d \geq 1$,
   (a) $\|\nabla I_1\|_{L^1} = \|\nabla I_2\|_{L^1}$, where L^1 denotes the space of integrable functions over D;
   (b) $\nabla I_1 \;//\; \nabla I_2 \circ f^*$.
   (c) relation $\sim$ defined by

$$[I_1 \sim I_2] \Longleftrightarrow [\exists f \ \xi\text{-rigid for } I_1 \text{ s.t. } I_1 = I_2 \circ f]$$

   is an equivalence relation on $C_0^1(D)$;
3. suppose $d = 2$: then,
   (a) if $Jac(f^*)$ is symmetric, then (7) means that if $|\nabla I_1| \neq 0$,

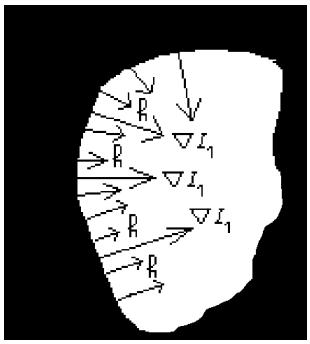

Fig. 3. An example of motion $h = f - Id$ of a ξ-rigid deformation f for image I_1. We show a level set of image I_1, and the fields ∇I_1 and h along its boundary. h varies only along the direction of ∇I_1.

- direction $\eta = \frac{\nabla I_1}{|\nabla I_1|}$ is eigenvector ($\lambda = det(Jac(f)$ is an eigenvalue);
- direction $\xi = \frac{\nabla I_1^{\perp}}{|\nabla I_1|}$ is "rigid" ($\lambda = 1$ is an eigenvalue);

This property can be seen as a non-sliding motion property. We illustrated this interesting property in Figure 3, where we show a level set of I_1, and a motion $h = f - Id$ of a ξ-rigid deformation f for image I_1. h can vary only along the direction of ∇I_1.

(b) $\kappa(I_1) = [Tr(Jac(f^*)) - det(Jac(f^*))].\kappa(I_2) \circ f^*$, where $\kappa(I)(x)$ stands for the curvature of the level line of I passing through x and $Tr(A)$ denotes the trace of matrix A;

4. if $d = 1$ or 2, and
   - h^* is known at
     - 1 point ($d = 1$).
     - each isolated critical point of I_1 and at one interior point of each connected constant set of I_1 ($d = 2$).
   - $h = h^*$ at this(ese) point(s), and

$$I_1 = I_2 \circ (Id + h) \text{ on } D,$$

then for all $x \in D$ where I_1 is not locally constant we have $h(x) = h^*(x)$.

Remark.
It is an important issue to know whether such h^* is unique. In case $d \in \{1, 2\}$, property 4 leads to uniqueness if h^* is known at some isolated points. Though it is not proved in the general case, we will assume uniqueness hereafter for simplicity.
As a consequence we can show that ξ-rigid deformations of images can be transfered to test functions. Indeed, we have the following

Lemma 1. *Suppose that*

1. I_1 *and* $I_2 \in C_0^1(D)$ *are such that:* $I_1 = I_2 \circ f$

2. *f is ξ-rigid for I_1*
3. *$\phi \in C^\infty(D;\mathbb{R})$, and $\Phi \in C^\infty(D;\mathbb{R}^d)$ s.t. $div\Phi = \phi$, where $C^\infty(D;\mathbb{R})$ denotes the space of indefinitely differentiable function from D to $\mathbb{R}$.*

Then, $\int_D (I_1 - I_2)\phi dx = \int_D < \nabla I_1, \Phi \circ f - \Phi > dx$.

Proof. See [20] ■

2.2 The Dirichlet operator

One choice for the set of test functions in Lemma 1 is the Fourier basis, the simplest projection onto which is the Dirichlet projection operator. Let $D = [-M, M]^d$; $S_\sigma = \{k \in Z^d, \forall i \in [1,d], |k_i| \leq M\sigma^2\}$; $c_k(I)$ denotes the Fourier coefficient of I defined by:

$$c_k(I) = \frac{1}{(2M)^{\frac{d}{2}}} \int_D I(x) e^{-\frac{i\pi < k,x >}{M}} dx.$$

Then the Dirichlet operator Π_σ is the linear mapping associating to each function $I \in C_0^1(D)$ the function $\Pi_\sigma(I) = G_\sigma * I$, where the convolution kernel G_σ is defined by its Fourier coefficients as follows:

$$c_k(G_\sigma) = \begin{cases} 1 \text{ if } k \in S_\sigma \\ 0 \text{ elsewhere} \end{cases}$$

2.3 New MCE by Linearization for the Dirichlet projection

Now that we have introduced our rigidity property of deformations and the Dirichlet projection, let us choose the test functions of Lemma 1 in the Fourier basis. Defining $P_\sigma^{I_1}(h^*)(x)$ through its Fourier coefficients:

$$c_k(P_\sigma^{I_1}(h^*)) = \begin{cases} \frac{1}{d} c_0(< \nabla I_1, h^* >) \text{ if } k = 0 \\ c_k(\frac{< \nabla I_1, k >< k, h^* >}{|k|^2}) \text{ if } k \in S_\sigma / \{0\} \\ 0 \text{ if } k \notin S_\sigma \end{cases}$$

we obtain the

Theorem 1. *If $f^* = Id + h^*$ is ξ-rigid for $I_1 = I_2 \circ f^* \in C_0^1(D)$, then we have:*

$$\|\Pi_\sigma(I_1 - I_2) - P_\sigma^{I_1}(h^*)\|_{L^2} \leq \frac{\pi}{2} \sigma^{d+2} \|h^* |\nabla I_1|^{\frac{1}{2}}\|_{L^2}^2.$$

This inequality is nothing but the sharpness of MCE (6):

$$\Pi_\sigma(I_1 - I_2)(x) \simeq P_\sigma^{I_1}(h^*)(x), \tag{8}$$

at scale σ. It clearly expresses the fact that measuring the motion (e.g perceiving the optical flow) h^* is not relevant outside of the support of $|\nabla I_1|$.
Proof. See [20] ■

3 Theoretical iterative scheme and convergence theorem

In section 2 we found a new MCE and showed that we can control the sharpness of it. In this section we will make a rather general assumption on the motion in the sense that it should belong to some linear parametric motion model without being more specific on the model basis functions. Though it is somewhat restrictive to have motion fields in a finite dimensional functional space, this structural hypothesis will be a key to bounding the residual motion norm after registration in order to iterate the process. This makes it possible to consider a constraint on motion when there is a priori knowledge (like for rigid motion) or consider multi-scale decomposition of motion for an iterative scheme.

3.1 Linear parametric motion models and least square estimation

Let us assume the motion h^* has to be in a finite dimensional space of deformation generated by basis functions $\Psi(x) = (\psi_i(x))_{i=1..n}$. Thus h^* can be decomposed in the basis: $\exists\ \Theta^* = (\theta_i^*)_{i=1..n}$ unique, such that:

$$h^*(x) =< \Psi(x), \Theta^* >= \sum_{i=1..n} \theta_i^* \psi_i(x),\ \forall x \in Supp(|\nabla I_1|).$$

MCE (6) viewed as a linear model writes:

$$\Pi_\sigma(I_1 - I_2) =< P_\sigma^{I_1}(\Psi), \Theta^* > .$$

Now set, for σ s.t. the $P_\sigma^{I_1}(\psi_i)$ be mutually linearly independent in L^2:

$$M_\sigma = P_\sigma^{I_1}(\Psi) \otimes P_\sigma^{I_1}(\Psi),\ \ Y_\sigma = \Pi_\sigma(I_1 - I_2),$$

where $\otimes$ stands for the tensorial product in L^2. Then applying basic results from the classical theory of linear models yields: $\hat{h} =< \Psi, \hat{\Theta} >=< \Psi, M_\sigma^{-1} B_\sigma >$, where column B_σ's components are defined by $(B_\sigma)_i =< P_\sigma^{I_1}(\psi_i), Y_\sigma >$.

3.2 Estimation error and residual motion

Given the least square estimation of the motion of last paragraph, we have

Lemma 2. *In this framework the motion estimation error is bounded by inequality*

$$\|(\hat{h} - h^*)|\nabla I_1|^{\frac{1}{2}}\|_{L^2} \leq \frac{\pi}{2}\sigma^{d+2}\left(Tr(M_\sigma^{-1}))\right)^{\frac{1}{2}} \|h^*|\nabla I_1|^{\frac{1}{2}}\|_{L^2}^2.$$

Proof. See [20] ■

If $Id + \hat{h}$ is invertible, we can define:

$$I_{1,1} = I_1 \circ \left(Id + \hat{h}\right)^{-1}. \tag{9}$$

Letting r_1 denote the residual motion such that $I_{1,1} = I_2 \circ (Id + r_1)$, if $Id + \hat{h}$ is ξ-rigid for I_1 then a variable change yields equality

$$\|(\hat{h} - h^*)|\nabla I_1|^{\frac{1}{2}}\|_{L^2} = \|r_1|\nabla I_{1,1}|^{\frac{1}{2}}\|_{L^2},$$

thus giving by Lemma 2 the following bound on the residual motion norm:

$$\|r_1|\nabla I_{1,1}|^{\frac{1}{2}}\|_{L^2} \leq \frac{\pi}{2}\sigma^{d+2}\Big(Tr(M_\sigma^{-1}))\Big)^{\frac{1}{2}}\|h^*|\nabla I_1|^{\frac{1}{2}}\|_{L^2}^2. \tag{10}$$

In view of equality (9) and inequality (10), iterating the motion estimation/registration process looks completely natural and allows for pointing out sufficient conditions for convergence of such a process. Indeed, provided the same assumptions are made at each step, relations (9) and (10) can be seen as recurrence ones, yielding both r_p and $I_{1,p}$ sequences.

3.3 Theoretical iterative scheme

Having control on the residual motion after one registration step, we deduce the following theoretical iterative motion estimation / registration scheme:

1. Initialization: Enter accuracy $\epsilon > 0$ and the maximal number of iterations N. Set $p = 0$, and $I_{1,0} = I_1$.
2. Iterate while $(\|I_{1,p} - I_2\| \geq \epsilon \ \& \ p \leq N)$
   (a) Enter the set of basis functions $\Psi_p = (\psi_{p,i})_{i=1..n_p}$ that linearly and uniquely decompose r_p on the support of $|\nabla I_{1,p}|$.
   (b) Enter scale σ_p and compute: $\hat{h}_p =< \Psi_p, M_{p,\sigma_p}^{-1} B_{\sigma_p} >$.
   (c) Set $I_{1,p+1} = I_{1,p} \circ (Id + \hat{h}_p)^{-1}$.

3.4 Convergence theorem

Now that we have designed an iterative motion estimation / registration scheme, let us infer sufficient conditions for the residual motion to vanish. This leads us to state our following main result:

Theorem 2. *If:*

1. *For all $p \geq 0$, $I_{1,p} \sim I_2$ (as defined in Section 2.1), and the residual motion r_p can be linearly and uniquely decomposed on a set of basis functions $\{\psi_{p,i}, i = 1..n_p\}$;*
2. *For all $p \geq 0$, there exists a scale $\sigma_p > 0$ such that the set of functions $\{P_{\sigma_p}^{I_{1,p}}(\psi_{p,i}), i = 1..n_p\}$ be free in L^2 and, for $p = 0$, we assume that :*

$$\|h^*|\nabla I_1|^{\frac{1}{2}}\|_{L^2} < \Big(\frac{\pi}{2}\sigma_0^{d+2} Tr(M_{0,\sigma_0})^{\frac{1}{2}}\Big)^{-1};$$

Set $C_0 = \Big(\frac{\pi}{2}\sigma_0^{d+2} Tr(M_{0,\sigma_0})^{\frac{1}{2}}\|h^*|\nabla I_1|^{\frac{1}{2}}\|_{L^2}\Big)^{-1}$;

3. *The sequence of conditioning ratios satisfy criteria:*
   $\forall p \geq 0$, $\frac{\sigma_{p+1}^{d+2} Tr(M_{p+1,\sigma_{p+1}})^{\frac{1}{2}}}{\sigma_p^{d+2} Tr(M_{p,\sigma_p})^{\frac{1}{2}}} \leq C_0$;
4. *For all $p \geq 0$, the estimated deformations $Id + \hat{h}_p \in Hom(D)$ and are ξ-rigid for $I_{1,p}$;*

Then, $\lim_{p\to\infty} \|r_p |\nabla I_{1,p}|^{1/2}\|_{L^2} = 0$.

Proof. See [20] ■

3.5 Numerical algorithm requirements

Firstly, due to the fact that h^* is unknown we have to make an arbitrary choice for the scale at each step. Secondly we at least have to ensure that $Id + \hat{h}$ be invertible at each step. Finally we are faced with the motion basis functions choice.

Multi-scale strategy The scale choice expresses both a priori knowledge on the motion range and its structure complexity. Here we assume that $(\sigma_p)_p$ is an increasing sequence, starting from $\sigma_0 > 0$ such that:

$$\#S_{\sigma_0} \geq \#\{\text{expected independent motions}\}. \tag{11}$$

Then let $\alpha \in]0,1[$. In order to justify the minimization problem at new scale $\sigma_{p+1} > \sigma_p$, we will choose it such that:

$$\|(\Pi_{\sigma_{p+1}} - \Pi_{\sigma_p})(I_{1,p+1} - I_2)\|_{L^2} > \alpha \|I_{1,p+1} - I_2\|_{L^2}, \tag{12}$$

Invertibility of $Id + \hat{h}_p$ Let $\beta > 0$. We will apply to $I_{1,p}$ the inverse of the maximal invertible linear part of the computed deformation e.g. $\left(Id + t^*.\hat{h}_p\right)^{-1}$, where

$$t^* = \sup_{t\in[0,1]} \{t \ / \ det(Jac(Id + t.\hat{h}_p)) \geq \beta\}. \tag{13}$$

Remark.
Recursive version of the algorithm

Set $f^*(I_1, I_2)$ the solution to the correspondence problem between I_1 and I_2. Then, $f^*(I_{1,p}, I_2) = f^*(I_{1,p+1}, I_2) \circ (Id + \hat{h}_p)$. We thus deduce the following alternate recursive motion estimation / registration function $f^*(I_1, I_2)$ defined by:

$$\begin{cases} \text{If } \|I_1 - I_2\| > \epsilon, \\ \text{Then} \begin{cases} \text{Calculate } \hat{h}(I_1, I_2) \\ \text{Deform: } I_{1,1} = I_1 \circ (Id + \hat{h}(I_1, I_2))^{-1} \\ \text{Call } f = f^*(I_{1,1}, I_2) \\ \text{Return } f \circ (Id + \hat{h}(I_1, I_2)) \end{cases} \\ \text{Else return } Id \end{cases}$$

Choosing the set of basis functions A major difficulty arising in the theoretical scheme comes from the lack of a priori knowledge on the finite set of basis functions to be entered at each step. To alleviate this problem we proposed two different approaches. In [20] we consider splitting both images into a collection of pairs of level sets to be matched. In Section 4 we will use an implicit approach via the optimal step gradient algorithm when minimizing the quadratic energy associated to MCE (6).

4 Implicit approach of basis functions

We now use the optimal step gradient algorithm for the minimization of the quadratic functional associated to MCE (6). There are at least two good reasons for doing this:

- the choice of base functions is implicit: it depends on the images I_1 and I_2, and the scale space.
- we can control and stop the quadratic minimization if the associated operator is no longer positive definite.

The general algorithm does not guaranty that the resulting matrix M_{p,σ_p} be invertible. Hence we suggest to systematically use a stopping criteria to control the quadratic minimization, based on the descent speed or simply a maximum number of iterations N_G.

In that case our final algorithm writes:

1. Initialization: Enter accuracy $\epsilon > 0$ and the maximal number of iterations N. Set $p = 0$, $I_{1,0} = I_1$, and choose first scale σ_0 according to (11).
2. Iterate while $(\|I_{1,p} - I_2\| \geq \epsilon \ \& \ p \leq N \ \& \ \sigma_p \leq 1)$
   (a) Choose σ_p satisfying (12).
   (b) Apply N_G iterations of the optimal step gradient algorithm for the minimization of

$$E_p(h) = \|\Pi_{\sigma_p}(I_{1,p} - I_2) - P_{\sigma_p}^{I_{1,p}}(h)\|_{L^2}^2.$$

   (c) Compute $I_{1,p+1} = I_{1,p} \circ (Id + t^*.\hat{h}_p)^{-1}$ with t^* defined by (13) and increment p.

In the following experiments we have fixed parameters to $\alpha = 2.5\%$, $N_G = 5$, $\beta = 0.1$.

Running the algorithm

We illustrate the algorithm on pairs of images with large deformation for registration applications and movies for motion estimation applications.

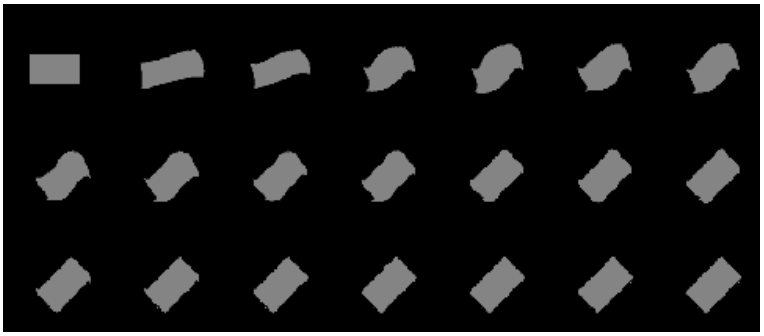

Fig. 4. Registration movie of a rotated rectangle: from left to right and from top to bottom we show the different steps of the algorithm performing the registration.

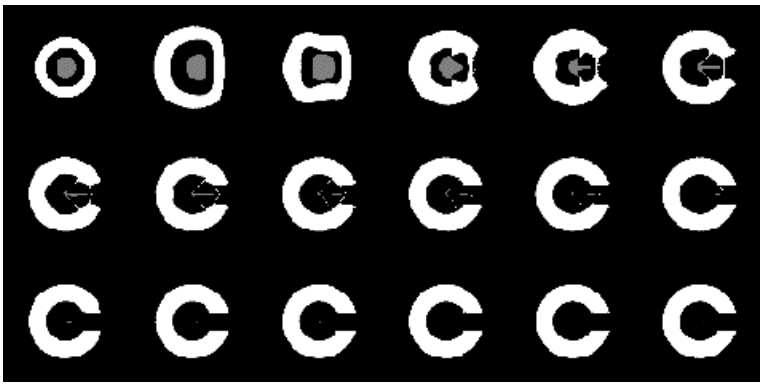

Fig. 5. Registration movie of a target to a 'C' letter. Again, each image corresponds to a step in the iterative scheme.

- **Registration problems involving large deformation**: In figures 4 and 5 we show the different steps of the algorithm performing the registration between the first and last images. In Figures 6 to 8, we show the study and target images, and the deformed study image after applying the estimated motion. This was applied for two examples of faces and a turbulence image featuring a vortex at two different states.
- **Optical Flow estimation examples**: in Figure 9 we show the sequence of the registered images of the original Cronkite sequence onto first image using the sequence of computed backward motions. The result is expected to be motionless. On top of Figure 10, we show the complete movie obtained by deforming iteratively only the first image of Cronkite movie. For that we use the sequence of computed motions between each pair of consecutive images of the original movie. In Figure 10 on the bottom, we see the error images.

Fig. 6. Scene registration example: Study image (left), deformed Study image onto Target image (center), and Target image (right).

Fig. 7. Registration of a face with two different expressions: Study image (left), deformed Study image onto Target image (center), and Target image (right).

5 Conclusion

We have addressed the theoretical problems of motion estimation and registration of images. We have introduced a new local ridigity hypothesis that we used to infer a unique Motion Constraint Equation with small remainder at coarse scales. We then showed that upon hypotheses on the motion norm and structure/scale tradeoff, an iterative motion estimation/registration scheme could converge towards the expected solution of the problem e.g. the global minimum of the nonlinear least square problem energy. Since each step of the theoretical scheme needs a set of motion basis functions which are not known, we have designed an implicit algorithm and illustrated the method with synthetic and real images, including large deformation examples.

References

1. L. Alvarez, J. Esclarin, M. Lefébure, J. Sanchez. A PDE model for computing the optical flow. *Proc. XVI Congresso de Ecuaciones Diferenciales y Aplicaciones*, Las Palmas, pp. 1349–1356, 1999.
2. L. Alvarez, J. Weickert, J. Sanchez, Reliable estimation of dense optical flow fields with large displacements. TR 2, Universidad de Las Palmas de Gran Canaria, November 1999.
3. G. Aubert, R. Deriche and P. Kornprobst. Computing optical flow via variational techniques. *SIAM J. Appl. Math.*, Vol. 60 (1), pp. 156–182, 1999.

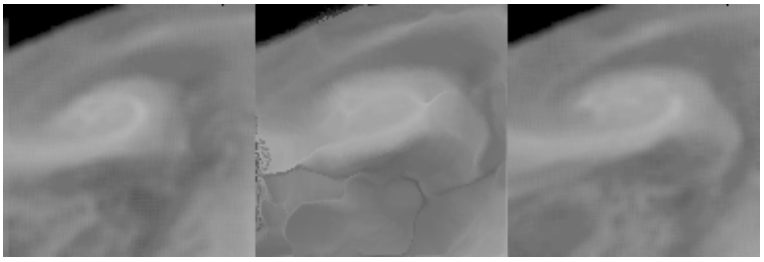

Fig. 8. Registration of a vortex at two different states: Study image (left), deformed Study image onto Target image (center), and Target image (right).

4. N. Ayache. Medical computer vision, virtual reality and robotics. IVC (13), No 4, May 1995, pp 295-313.
5. Ruzena Bajcsy and Stane Kovacic. Multiresolution elastic matching. CVGIP, (46), No 1, pp. 1–21, 1989.
6. J.L. Barron, D.J. Fleet, and S.S. Beauchemin. Performance of optical flow. IJCV, 12(1):43–77, 1994.
7. M. Ben-Ezra, B. Rousso, and S. Peleg. Motion segmentation using convergence properties. In *ARPA Im. Unders. Workshop*, pp II 1233-1235, 1994.
8. J.R. Bergen and E.H. Adelson. Hierarchical, computationally efficient motion estimation algorithm. *J. of the Optical Society Am.*, 4(35), 1987.
9. C. Bernard. Discrete wavelet analysis: a new framework for fast optic flow computation. *ECCV*, 1998.
10. M. Black and A. Rangajaran. On the unification of line processes, outlier rejection and robust statistics with applications in early vision. IJCV, Vol. 19, 1996.
11. P. Bouthemy and J.M. Odobez. Robust multiresolution estimation of parametric motion models. *J. of Vis. Comm. and Image Repres.*, 6(4):348–365, 1995.
12. M. Bro-Nielsen and C. Gramkow. Fast fluid registration of medical images. *VBC'96* Springer LNCS 1131, Hamburg, Germany, pp 267–276, Sept. 1996.
13. G. Christensen, R.D. Rabbitt, and M.I. Miller. 3D brain mapping using a deformable neuroanatomy. *Physics in Med and Biol*, (39), March :609–618, 1994.
14. D. Fleet, M. Black, Y. Yacoob and A. Jepson. Design and use of linear models for image motion analysis. *IJCV*, 36(3), 2000.
15. B. Galvin, B. McCane, K. Novins, D. Mason and S. Mills. Recovering Motion fields: An analysis of eight optical flow algorithms, *BMVC'98*, Sept. 1998.
16. P.R. Giaccone, D. Greenhill, G.A. Jones. Recovering very large visual motion fields. *SCIA97*, pp 917-922.
17. B.K.P. Horn and Brian Schunck. Determining optical flow. *Artificial Intelligence*, (17) (1-3) :185–204, 1981.
18. M. Irani, B. Rousso, and S. Peleg. Detecting and tracking multiple moving objects using temporal integration. In *ECCV92*, pp 282–287, 1992.
19. M. Lefébure Estimation de Mouvement et Recalage de Signaux et d'Images: Formalisation et Analyse. PhD Thesis, Université Paris-Dauphine, 1998.
20. M. Lefébure and L. D. Cohen. Image Registration, Optical Flow and Local Rigidity. CEREMADE Technical Report, 0102, January 2001. To appear in Journal of Mathematical Imaging and Vision, 14 (2):131–147, March 2001.
21. E. Mémin and P. Pérez. Dense estimation and object-based segmentation of the optical flow with robust techniques. IEEE Trans. IP, 1998.
22. S. Srinivasan, R. Chellappa. Optical flow using overlapped basis functions for solving global motions problems. In *ECCV98*, pp 288–304, 1998.
23. C. Stiller and J. Konrad. Estimating motion in image sequences. In *IEEE Signal Processing Magazine*, Vol. 16, July, pp 70–91, 1999.
24. D. Terzopoulos. Multiresolution algorithms in computational vision. *Image Understanding*. S. Ullman, W. Richards, 1986.
25. J.P. Thirion. Fast non-rigid matching of 3D medical images. Technical Report 2547, INRIA, 1995.

Fig. 9. Registered sequence of the original sequence onto first image using the computed backward motions.

26. A. Trouvé. Diffeomorphisms groups and pattern matching in image analysis. IJCV, 28(3), 1998.
27. B. C. Vemuri, J. Ye, Y. Chen and C. M. Leonard. A level-set based approach to image registration. *Proc. IEEE Workshop on Mathematical Methods in Biomedical Image Analysis, MMBIA'00*, Hilton Head Island, South Carolina, pp. 86–93, June 11-12 2000.
28. J. Weickert. On discontinuity-preserving optic flow. *Proc. Computer Vision and Mobile Robotics Workshop*, Santorini, pp. 115–122, Sept. 1998.
29. G. Whitten. A framework for adaptive scale space tracking solutions to problems in computational vision. In *ICCV'90, Osaka*, pp 210–220, Dec 1990.
30. A. Witkin, D. Terzopoulos, M. Kass. Signal matching through scale space. IJCV, 1(2):133–144, 1987.

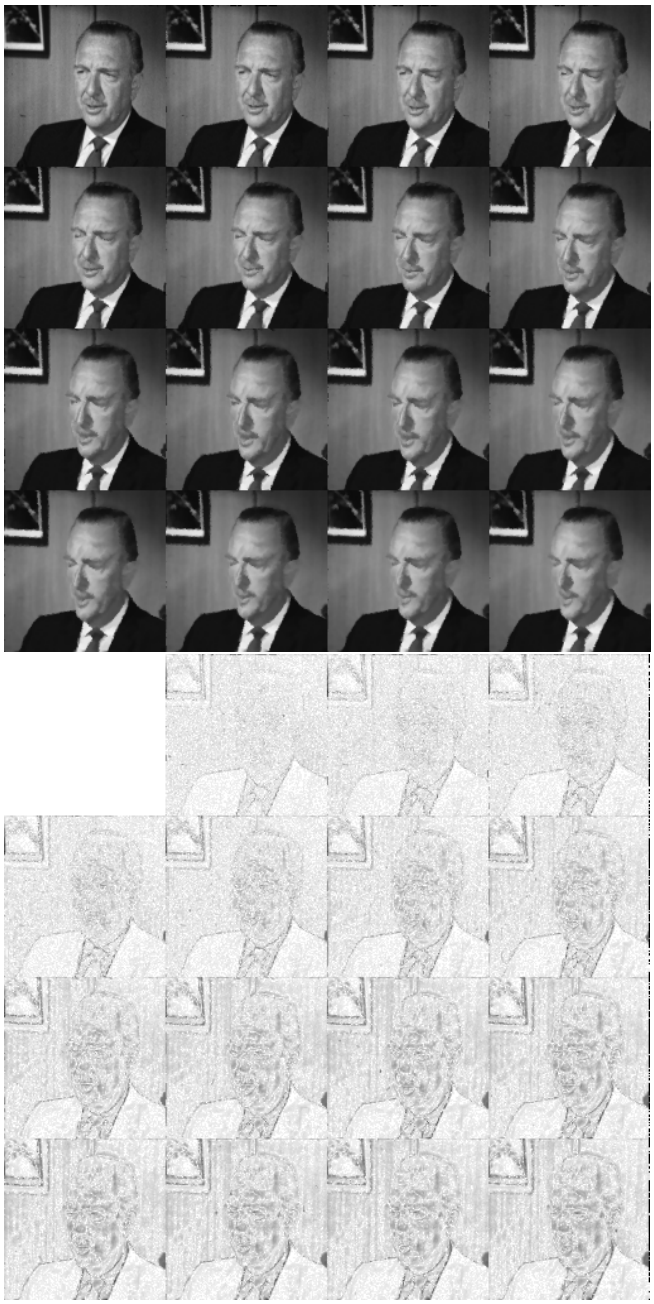

Fig. 10. On top, movie obtained by deforming only the first image of Cronkite movie using the sequence of computed motions. On the bottom, enhanced (applying $I' = 255.(1 - \sqrt{I/255})$) absolute difference between original and artificially deformed Cronkite sequences.